

Free-fall Frame Black Hole in Gravity's Rainbow

Jun Tao,^{*} Peng Wang,[†] and Haitang Yang[‡]

Center for Theoretical Physics, College of Physical Science and Technology,

Sichuan University, Chengdu, 610064, China

Abstract

Doubly special relativity (DSR) is an effective model for encoding quantum gravity in flat space-time. To incorporate DSR into general relativity, one could use “Gravity’s rainbow”, where the spacetime background felt by a test particle would depend on its energy. In this scenario, one could rewrite the rainbow metric $g_{\mu\nu}(E)$ in terms of some orthonormal frame fields and use the modified equivalence principle to determine the energy dependence of $g_{\mu\nu}(E)$. Obviously, the form of $g_{\mu\nu}(E)$ depends on the choice of the orthonormal frame. For a static black hole, there are two natural orthonormal frames, the static one hovering above it and freely falling one along geodesics. The cases with the static orthonormal frame have been extensively studied by many authors. The aim of this paper is to investigate properties of rainbow black holes in the scenario with the free-fall orthonormal frame. We first derive the metric of rainbow black holes and their Hawking temperatures in this free-fall scenario. Then, the thermodynamics of a rainbow Schwarzschild black hole is studied. Finally, we use the brick wall model to compute the thermal entropy of a massless scalar field near the horizon of a Schwarzschild rainbow black hole in this free-fall scenario.

^{*}Electronic address: taojun@scu.edu.cn

[†]Electronic address: pengw@scu.edu.cn

[‡]Electronic address: hyanga@scu.edu.cn

Contents

I. Introduction	2
II. Free-fall Frame Rainbow Black Hole	5
III. Thermodynamics of Rainbow Schwarzschild Black Hole	8
IV. Entropy of Rainbow Schwarzschild Black Hole in Brick Wall Model	11
V. Discussion and Conclusion	15
Acknowledgments	16
References	16

I. INTRODUCTION

It is generally believed that the framework of the smooth manifold and metric of classical general relativity breaks down at very high energy scales. Although a full theory of quantum gravity has yet to be available, there are various attempts using effective models to address this problem. Doubly Special Relativity (DSR) [1–4] is one of them, where the non-linear Lorentz transformation in momentum spacetime is proposed to make the Planck length as a new invariant scale. One of its predictions is that the transformation laws of special relativity are modified at very high energies. Thus, the energy-momentum dispersion relation for a particle of mass m could be modified to

$$E^2 f^2(E/m_p) - p^2 g^2(E/m_p) = m^2, \quad (1)$$

where m_p is the Planck mass, and $f(x)$ and $g(x)$ are two general functions with the following properties:

$$\lim_{x \rightarrow 0} f(x) = 1 \text{ and } \lim_{x \rightarrow 0} g(x) = 1. \quad (2)$$

The modified dispersion relation (MDR) might play an important role in astronomical and cosmological observations, such as the threshold anomalies of ultra high energy cosmic rays and TeV photons [5–10]. One of the popular choice for the functions $f(x)$ and $g(x)$ has

been proposed by Amelino-Camelia et al. [11, 12], which gives

$$f(x) = 1 \text{ and } g(x) = \sqrt{1 - \eta x^n}. \quad (3)$$

Usually one has $n > 0$. As shown in [12], this formula is compatible with some of the results obtained in the Loop-Quantum-Gravity approach and reflects the results obtained in κ -Minkowski and other noncommutative spacetimes. Phenomenological implications of this “Amelino-Camelia (AC) dispersion relation” are also reviewed in [12].

To incorporate DSR into the framework of general relativity, Magueijo and Smolin [13] proposed the “Gravity’s rainbow”, where the spacetime background felt by a test particle would depend on its energy. Consequently, the energy of the test particle deforms the background geometry and hence the dispersion relation. As regards the metric, it would be replaced by a one parameter family of metrics which depends on the energy of the test particle, forming a “rainbow metric”. Specifically, for the energy-independent metric given by

$$d\tilde{s}^2 = \tilde{g}_{\mu\nu} dx^\mu \otimes dx^\nu, \quad (4)$$

we could rewrite it in terms of a set of energy-independent orthonormal frame fields \tilde{e}_a :

$$d\tilde{s}^2 = \eta^{ab} \tilde{e}_a \otimes \tilde{e}_b. \quad (5)$$

Thus, the rainbow modified equivalence principle [13] implies that the energy-dependent rainbow counterpart for the energy-independent metric (4) is given by

$$ds^2 = \eta^{ab} e_a \otimes e_b, \quad (6)$$

where the energy-dependent frame fields are

$$e_0 = \frac{\tilde{e}_0}{f(E/m_p)} \text{ and } e_i = \frac{\tilde{e}_i}{g(E/m_p)}. \quad (7)$$

Note that the MDR (1) was considered in [13]. Let see how this works in an example, a static black hole with the line element

$$d\tilde{s}^2 = B(r) dt^2 - \frac{dr^2}{B(r)} - C(r^2) h_{\alpha\beta}(x) dx^\alpha dx^\beta, \quad (8)$$

where we assume that the black hole is asymptotically flat which gives $B(r) \rightarrow 1$ as $r \rightarrow \infty$.

There are many choices for \tilde{e}_a , but one obvious one:

$$\tilde{e}_0 = \sqrt{B(r)} dt, \quad \tilde{e}_r = \frac{dr}{\sqrt{B(r)}}, \text{ and } \tilde{e}_j, \quad (9)$$

where \tilde{e}_i are some set of one-forms such that $\delta^{ij}\tilde{e}_i \otimes \tilde{e}_j = C(r^2) h_{\alpha\beta}(x) dx^\alpha dx^\beta$. Therefore, the corresponding rainbow metric is

$$ds^2 = \eta^{ab} e_a \otimes e_b = \frac{B(r)}{f^2(E/m_p)} dt^2 - \frac{dr^2}{g^2(E/m_p) B(r)} - \frac{C(r^2) h_{\alpha\beta}(x) dx^\alpha dx^\beta}{g^2(E/m_p)}. \quad (10)$$

For $B(r) = 1 - \frac{2GM}{r}$ and $C(r^2) h_{\alpha\beta}(x) dx^\alpha dx^\beta = r^2 d\Omega^2$, eqn. (10) gives the rainbow Schwarzschild metric, which was also obtained in [13] using Birkhoff's theorem.

The orthonormal frame adopted in eqn. (9) is a static frame which is anchored to observers hovering above the black hole. The energy and momentum measured by the static observers would satisfy the MDR (1) in the rainbow metric (10). This rainbow metric (10) has received a lot of attention and some relevant work can be found in [14–21]. However, another natural choice for the orthonormal frame is the one anchored to freely falling observers along the radial direction. For the energy-independent metric (8), it is obvious that different choice of orthonormal frame could lead to different form of the rainbow counterpart. Actually, in section II we will show that the rainbow black hole obtained using the free-fall orthonormal frame is given by

$$ds^2 = \frac{dt_p^2}{f^2(E/m_p)} - \frac{[dr - v(r) dt_p]^2}{g^2(E/m_p)} - \frac{C(r^2) h_{\alpha\beta}(x) dx^\alpha dx^\beta}{g^2(E/m_p)} \quad (11)$$

where $v(r) = -\sqrt{1 - B(r)}$ and t_p is given in eqn. (15). In what follows, we will refer to the rainbow black holes (10) and (11) as Static Frame (SF) and Free-fall Frame (FF) rainbow black holes, respectively.

In this paper, we aim to explore thermodynamics of FF rainbow black holes. For the static black hole (8), its SF and FF rainbow counterparts could lead to quite different physics. In the following sections, we find that

1. For a test particle, the position of the event horizon of the FF rainbow black hole (11) is always energy dependent, which can be obtained by solving eqn. (19). However, for the SF one (10), it is obvious that the event horizon radius r_h is energy independent, which is given by $B(r_h) = 0$.
2. The effective Hawking temperature of the SF rainbow black hole (10) is [22]

$$T_h = T_0 \frac{g(E/m_p)}{f(E/m_p)}, \quad (12)$$

where T_0 is the standard Hawking temperature. For the FF one (11), the effective Hawking temperature is given by eqn. (26). In such case, due to the complicated expression for r_h , the expression for T_h is usually more complex than eqn. (12). However, for a FF rainbow Schwarzschild black hole, it shows that the effective Hawking temperature is

$$T_h = T_0 \frac{g^3(E/m_p)}{f^3(E/m_p)}. \quad (13)$$

3. Thermodynamics of SF and FF rainbow black holes are thus different. Specifically, for the AC dispersion relation (3), we find that the behaviors of SF and FF rainbow Schwarzschild black holes during the final stage of evaporation process are dramatically different for $\eta < 0$ and $\frac{2}{3} \leq n \leq 2$. For example, a remnant exists for the FF black hole while it does not for the SF one in the case with $\eta < 0$ and $n = \frac{2}{3}$. More discussions can be found in section V.

The remainder of our paper is organized as follows. In section II, the metric of a FF rainbow black hole is derived, and its Hawking temperature is obtained using the Hamilton-Jacobi method. The temperature and entropy of a FF rainbow Schwarzschild black hole are computed in section III. In section IV, we calculate the atmosphere entropy of a massless scalar field near the horizon of a FF rainbow Schwarzschild black hole using the brick wall model. Section V is devoted to our discussion and conclusions. Throughout the paper we take Geometrized units $c = G = 1$, where the Planck constant \hbar is square of the Planck mass m_p .

II. FREE-FALL FRAME RAINBOW BLACK HOLE

The coordinate used in eqn. (8) is the Schwarzschild-like one, where the line element is diagonal. However, a more suitable coordinate for describing a specific family of freely falling observers is the Painleve-Gullstrand (PG) coordinate [23, 24]. The PG coordinate anchored to the freely falling observers along the radial direction takes the form of

$$ds^2 = dt_p^2 - [dr - v(r) dt_p]^2 - C(r^2) h_{\alpha\beta}(x) dx^\alpha dx^\beta, \quad (14)$$

where $v(r)$ is the velocity of the free fall observers with respect to the rest observer and t_p measures proper time along them. We assume $v < 0$, $dv/dr > 0$ and $v \rightarrow v_0 \leq 0$ as $r \rightarrow \infty$.

Note that $v < 0$ means the infalling observers. For simplicity we specialize to the particular family of observers with $v_0 = 0$ who start at infinity with a zero initial velocity. Comparing the vector field of the freely falling observers in PG and Schwarzschild-like coordinates, we find

$$\begin{aligned} t_p &= t + \int \frac{\sqrt{1 - B(r)}}{B(r)} dr, \\ v(r) &= -\sqrt{1 - B(r)}. \end{aligned} \quad (15)$$

Requiring $\tilde{e}_0 = dt_p$, we can easily find that the one-forms \tilde{e}_a for the free-fall orthonormal frame are given by

$$\tilde{e}_0 = dt_p, \quad \tilde{e}_r = dr - v(r) dt_p, \quad \text{and} \quad \tilde{e}_j, \quad (16)$$

where $\delta^{ij} \tilde{e}_i \otimes \tilde{e}_j = C(r^2) h_{\alpha\beta}(x) dx^\alpha dx^\beta$.

In the context of rainbow gravity, the corresponding energy-independent metric is

$$\begin{aligned} ds^2 &= \frac{\tilde{e}_0 \otimes \tilde{e}_0}{f^2(E/m_p)} - \frac{\tilde{e}_r \otimes \tilde{e}_r + \delta^{ij} \tilde{e}_i \otimes \tilde{e}_j}{g^2(E/m_p)} \\ &= \frac{dt_p^2}{f^2(E/m_p)} - \frac{[dr - v(r) dt_p]^2}{g^2(E/m_p)} - \frac{C(r^2) h_{\alpha\beta}(x) dx^\alpha dx^\beta}{g^2(E/m_p)}. \end{aligned} \quad (17)$$

The event horizon $r = r_h$ will be at which g^{rr} vanishes:

$$g^{rr}(r_h) = v^2(r_h) f^2(E/m_p) - g^2(E/m_p) = 0, \quad (18)$$

which leads to

$$B(r_h) = 1 - \frac{g^2(E/m_p)}{f^2(E/m_p)}. \quad (19)$$

It is interesting to note that the position of the event horizon depends on the energy E for FF rainbow black holes while it does not for SF ones.

We now use the Hamilton-Jacobi method to calculate the Hawking temperature of the FF rainbow black hole (11). After the Hawking's original derivation, there have been some other methods proposed to understand the Hawking radiation. Recently, a semiclassical method of modeling Hawking radiation as a tunneling process has been developed and attracted a lot of attention. This method was first proposed by Kraus and Wilczek [25, 26], which is known as the null geodesic method. Later, the tunneling behaviors of particles were investigated using the Hamilton-Jacobi method [27–29]. In the Hamilton-Jacobi method, one ignores the self-gravitation of emitted particles and assumes that their action satisfies the relativistic

Hamilton-Jacobi equation. The tunneling probability for the classically forbidden trajectory from inside to outside the horizon is obtained by using the Hamilton-Jacobi equation to calculate the imaginary part of the action for the tunneling process.

In [30], it has been shown that the Hamilton-Jacobi equations for massless scalars, spin 1/2 fermions and vector bosons in the rainbow metric $ds^2 = \tilde{g}_{\mu\nu}(E) dx^\mu dx^\nu$ are all given by

$$\tilde{g}_{\mu\nu}(E) \partial^\mu I \partial^\nu I = 0, \quad (20)$$

where I is the tunnelling particle's action. From eqn. (20), one finds that the Hamilton-Jacobi equation for a massless particle in the rainbow metric (11) becomes

$$f^2(E/m_p) [\partial_{t_p} I + v(r) \partial_r I]^2 = g^2(E/m_p) \left[(\partial_r I)^2 + \frac{h^{\alpha\beta}(x) (\partial_\alpha I) (\partial_\beta I)}{C(r^2)} \right]. \quad (21)$$

To solve the Hamilton-Jacobi equation for the action I , we can employ the following ansatz

$$I = -Et_p + W(r) + \Theta(x), \quad (22)$$

where E is the particle's energy. Plugging the ansatz into eqn. (21), we have differential equations for $W(r)$ and $\Theta(x)$:

$$\begin{aligned} h^{\alpha\beta}(x) \partial_\alpha \Theta(x) \partial_\beta \Theta(x) &= \lambda, \\ p_r^\pm \equiv \partial_r W_\pm(r) &= \frac{-C(r^2) v(r) E \pm C(r^2) \sqrt{E^2 \frac{g^2(E/m_p)}{f^2(E/m_p)} + \frac{\lambda}{C(r^2)} \left[v^2(r) - \frac{g^2(E/m_p)}{f^2(E/m_p)} \right] \frac{g^2(E/m_p)}{f^2(E/m_p)}}}}{C(r^2) \left[\frac{g^2(E/m_p)}{f^2(E/m_p)} - v^2(r) \right]}, \end{aligned} \quad (23)$$

where $+/-$ denotes the outgoing/ingoing solutions and λ is a constant. Using the residue theory for the semi circle around $r = r_h$, we get

$$\begin{aligned} \text{Im } W_+(r) &= \frac{2\pi}{B'(r_h)} \frac{g(E/m_p)}{f(E/m_p)} E, \\ \text{Im } W_-(r) &= 0. \end{aligned} \quad (24)$$

As shown in [31], the probability of a particle tunneling from inside to outside the horizon is

$$P_{emit} \propto \exp \left[-\frac{2}{\hbar} (\text{Im } W_+ - \text{Im } W_-) \right]. \quad (25)$$

There is a Boltzmann factor in P_{emit} with an effective Hawking temperature, which is

$$T_h = \frac{\hbar B'(r_h)}{4\pi} \frac{f(E/m_p)}{g(E/m_p)}, \quad (26)$$

where we take $k_B = 1$.

III. THERMODYNAMICS OF RAINBOW SCHWARZSCHILD BLACK HOLE

In this section, for simplicity we consider a FF rainbow Schwarzschild black hole of mass M with $B(r) = 1 - \frac{2M}{r}$ in eqn. (11). For the FF rainbow Schwarzschild black hole, eqn. (19) gives the position of the event horizon:

$$r_h = 2M \frac{f^2(E/m_p)}{g^2(E/m_p)}. \quad (27)$$

Thus, eqn. (26) leads to the effective Hawking temperature:

$$T_h = T_0 \frac{g^3(E/m_p)}{f^3(E/m_p)}, \quad (28)$$

where $T_0 = \frac{\hbar}{8\pi M}$.

As in [30], the Heisenberg uncertainty principle can be used to estimate the black hole's temperature. The Heisenberg uncertainty principle gives a relation between the momentum p of an emitted particle and the event horizon radius r_h of the black hole [32, 33]:

$$p/m_p \sim \delta p/m_p \sim \hbar/m_p \delta x \sim m_p/r_h. \quad (29)$$

Assuming that the emitted particle is massless, we find that the modified dispersion relation (1) becomes

$$\frac{E}{m_p} \frac{f(E/m_p)}{g(E/m_p)} = \frac{p}{m_p}. \quad (30)$$

Substituting eqn. (27) into eqn. (29) and using eqn. (30), we have for the energy of the particle:

$$x \frac{f^3(x)}{g^3(x)} = y, \quad (31)$$

where $x \equiv E/m_p$ and $y \equiv \frac{m_p}{2M}$. To express the black hole's temperature in terms of M , one can solve eqn. (31) for x in terms of y . In fact, the solution for x can be expressed as

$$x = yh(y), \quad (32)$$

where eqn. (31) is inverted to obtain the function $h(y)$ and $\lim_{y \rightarrow 0} h(y) = 1$. Substituting eqn. (32) into eqn. (28) gives the black hole's temperature:

$$T_{BH} = T_0 \frac{x}{y} = T_0 h\left(\frac{m_p}{2M}\right). \quad (33)$$

The range of the left-hand side (LHS) of eqn. (31) determines the ranges of the values of M . Specifically, the maximum value of the LHS of eqn. (31), which is denoted by y_{cr} , gives

that $M \geq \frac{m_p}{2y_{cr}}$. If y_{cr} is finite, it predicts the existence of the black hole's remnant. For some functions $f(x)$ and $g(x)$, the domain of the LHS of eqn. (31) might be $[0, x_{cr}]/[0, x_{cr})$ with x_{cr} being finite. Thus, it gives that the energy of the particle $E \leq m_p x_{cr}$. If the domain is $[0, \infty)$, we simply set $x_{cr} = \infty$.

For the AC dispersion relation given in eqn. (3), eqn. (30) becomes

$$\frac{x}{(1 - \eta x^n)^{\frac{3}{2}}} = y. \quad (34)$$

If $\eta > 0$, one finds that $y_{cr} = 0$. However, there is an upper bound $x_{cr} = \eta^{-1/n}$ on x to make the LHS of eqn. (34) real. If $\eta < 0$, $x_{cr} = \infty$ and $y_{cr} = \infty$ for $0 < n < \frac{2}{3}$, and $x_{cr} = \infty$ and $y_{cr} = |\eta|^{-3/2}$ for $n = \frac{2}{3}$. For the case with $\eta < 0$ and $n > \frac{2}{3}$, the LHS of eqn. (34) has a global maximum value y_0 at x_0 , where we define

$$\begin{aligned} x_0 &\equiv \left(\frac{2-3n}{2} \eta \right)^{-\frac{1}{n}}, \\ y_0 &\equiv \left(\frac{3n-2}{3n} \right)^{\frac{3}{2}} \left(\frac{2-3n}{2} \eta \right)^{-\frac{1}{n}}. \end{aligned} \quad (35)$$

Thus, it would appear that $y \leq y_0$ and $x < \infty$ since x can go to infinity. However, as argued in [30, 34], the "runaways" solution to eqn. (34), which does not exist in the limit of $\eta \rightarrow 0$, should be discarded. In this case, we have $x_{cr} = x_0$ instead of $x_{cr} = \infty$. We list x_{cr} and y_{cr} for various choices of n and η in TABLE I. If $y \ll 1$, one has $x \ll 1$, and hence eqn. (34) becomes

$$y = x \left(1 + \frac{3\eta x^n}{2} + \mathcal{O}(x^{2n}) \right), \quad (36)$$

which gives

$$h(y) = 1 - \frac{3\eta y^n}{2} + \mathcal{O}(y^{2n}). \quad (37)$$

Thus for $M \gg m_p$, we have from eqn. (37) that

$$T_{BH} = \frac{m_p^2}{8\pi M} \left[1 - \frac{3\eta}{2^{n+1}} \frac{m_p^n}{M^n} + \mathcal{O}\left(\frac{m_p^{2n}}{M^{2n}}\right) \right]. \quad (38)$$

The minimum mass M_{cr} of the black hole is given by

$$M_{cr} = \frac{m_p}{2y_{cr}}. \quad (39)$$

When the mass M reaches M_{cr} , the final temperature of the black hole is denoted by T_{BH}^{cr} .

Eqn. (33) gives that

$$T_{BH}^{cr} = \frac{x_{cr} m_p}{4\pi}. \quad (40)$$

For $\eta < 0$ and $n \geq \frac{2}{3}$, y_{cr} is finite, and hence the black hole would have non-vanishing minimum mass M_{cr} . This implies the existence of the black hole's remnant due to rainbow gravity. By eqn. (40), we find that T_{BH}^{cr} is infinite for $n = \frac{2}{3}$ while T_{BH}^{cr} is $\frac{x_0 m_p}{4\pi}$ for $n > \frac{2}{3}$. For $\eta < 0$ and $0 < n < \frac{2}{3}$, we find that $M_{cr} = 0$ and $T_{BH}^{cr} = \infty$. In this case, the black hole would evaporate completely while its temperature increases and finally becomes infinity during evaporation, just like the standard Hawking radiation. For $\eta > 0$, the black hole would also evaporate completely. However, the temperature of the black hole is a finite value $\frac{\eta^{-1/n} m_p}{4\pi}$ at the end of the evaporation process. We list M_{cr} and T_{BH}^{cr} for all the possible values of η and n in TABLE I. In FIG. 1, we plot the temperature T_{BH}/m_p against the black hole mass M/m_p , for examples with $(\eta, n) = (1, 1)$, $(\eta, n) = (-1, \frac{1}{2})$, $(\eta, n) = (-1, \frac{2}{3})$, and $(\eta, n) = (-1, 1)$. The standard Hawking radiation is also plotted as a blue line in FIG. 1.

Using the first law of black hole thermodynamics $dS_{BH} = dM/T_{BH}$, we find that the entropy of the black hole is

$$S_{BH} = \int_{M_{cr}}^M \frac{dM}{T_{BH}} = 2\pi \int_{\frac{m_p}{2M}}^{y_{cr}} \frac{dy}{y^3 h(y)}, \quad (41)$$

where $y_{cr} = \frac{m_p}{2M_{cr}}$. For the usual case, we have $h(y) = 1$ and $y_{cr} = \infty$. Thus, eqn. (41) gives the Bekenstein-Hawking entropy

$$S_{BH} = \frac{4\pi M^2}{m_p^2} = \frac{A}{4\hbar}. \quad (42)$$

where $A = 4\pi (2M)^2$ is the horizon area of the usual Schwarzschild black hole. If $M \gg m_p$ ($A \gg \hbar$), eqn. (41) gives the entropy up to the subleading term

$$S_{BH} \sim \begin{cases} \frac{A}{4\hbar} + \frac{3\pi\eta}{2-n} \left(\frac{A}{4\pi\hbar}\right)^{\frac{2-n}{2}} & n \neq 2 \\ \frac{A}{4\hbar} + \frac{3\pi\eta}{2} \ln \frac{A}{4\pi\hbar} & n = 2 \end{cases}, \quad (43)$$

	x_{cr}	y_{cr}	M_{cr}	T_{BH}^{cr}/m_p	Lines in figures
$\eta = 0$	∞	∞	0	∞	Blue Solid
$\eta > 0$	$\eta^{-1/n}$	∞	0	$\frac{\eta^{-1/n}}{4\pi}$	Black Solid
$\eta < 0, 0 < n < \frac{2}{3}$	∞	∞	0	∞	Black Dashed
$\eta < 0, n = \frac{2}{3}$	∞	$ \eta ^{-\frac{3}{2}}$	$\frac{m_p \eta ^{\frac{3}{2}}}{2}$	∞	Red Dashed
$\eta < 0, n > \frac{2}{3}$	x_0	y_0	$\frac{m_p}{2y_0}$	$\frac{x_0}{4\pi}$	Red Solid

TABLE I: The values of x_{cr} , y_{cr} , M_{cr} , and T_{BH}^{cr}/m_p for a FF rainbow Schwarzschild black hole.

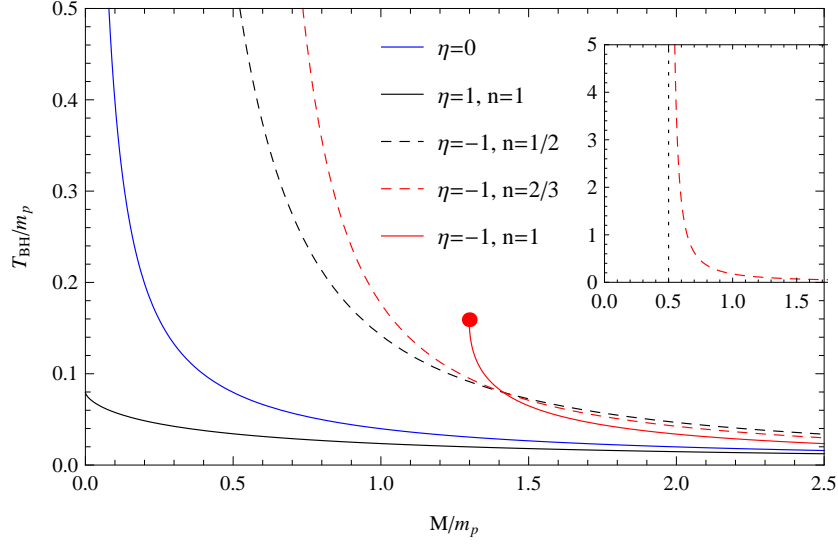


FIG. 1: Plot of the temperature T_{BH}/m_p against the mass M/m_p for a FF rainbow Schwarzschild black hole. All the lines asymptotically approach $T_{BH} = 0$ as $M/m_p \rightarrow \infty$. The blue line is the usual case, where T_{BH} blows up as $M \rightarrow 0$. The red dot is the end of the red solid line, where the black hole has a remnant $M_{cr} = \frac{3\frac{3}{2}}{4}m_p$. In this case, T_{BH} does not blow up as $M \rightarrow M_{cr}$. The black dotted line is the asymptotic line of the red dashed line as $M \rightarrow M_{cr} = 0.5m_p$, which is the black hole's remnant. In this case, T_{BH} blows up as $M \rightarrow M_{cr}$.

where we use eqn. (37) for $h(y)$. The leading terms of eqn. (43) are the familiar Bekenstein-Hawking entropy. For $n = 2$, we obtain the logarithmic subleading term. In FIG. 2, we plot the entropy S against the black hole mass M/m_p , for examples with $\eta = 0$, $(\eta, n) = (1, 1)$, $(\eta, n) = (-1, \frac{1}{2})$, $(\eta, n) = (-1, \frac{2}{3})$, and $(\eta, n) = (-1, 1)$.

IV. ENTROPY OF RAINBOW SCHWARZSCHILD BLACK HOLE IN BRICK WALL MODEL

Although all the evidences suggest that the Bekenstein-Hawking entropy is the thermodynamic entropy, the statistical origin of black holes' entropy has not yet been fully understood. One of candidate for the statistical origin is the entropy of the thermal atmosphere of black holes. However, when one attempts to calculate the entropy of the thermal atmosphere, there are two kinds of potential divergences. The first one arises from infinite volume of the system, which has to do with the contribution from the vacuum surrounding the system at

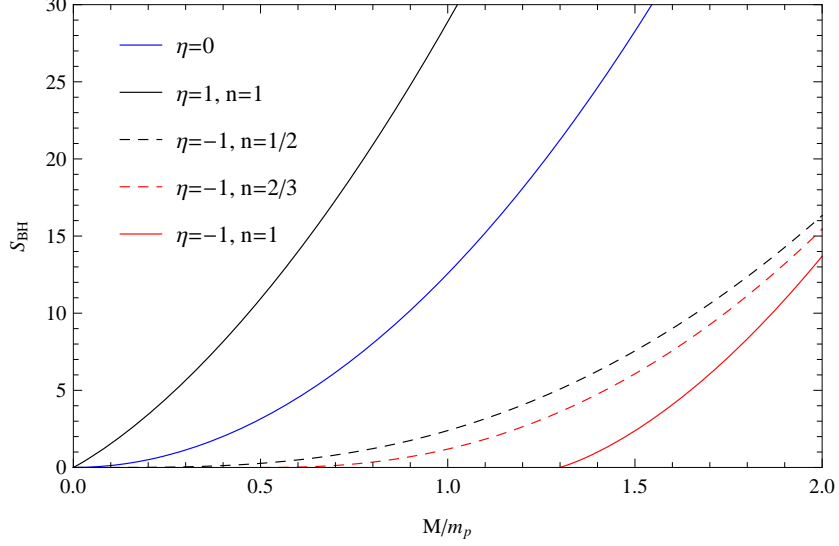


FIG. 2: Plot of the entropy S_{BH} against the mass M/m_p for a FF rainbow Schwarzschild black hole.

large distances and is of little relevance here. The second one is due to the infinite volume of the deep throat region near the horizon. To regulate the divergences, t' Hooft [35] proposed the brick wall model for a scalar field ϕ , where two brick wall cutoffs are introduced at some small distance r_ε from the horizon and at a large distance $L \gg r_h$,

$$\phi = 0 \quad \text{at } r = r_h + r_\varepsilon \text{ and } r = L. \quad (44)$$

In this section, we will use the brick wall model to calculate the entropy of a scalar field for a FF rainbow Schwarzschild black hole with $B(r) = 1 - \frac{2M}{r}$ in eqn. (11).

For particles emitted in a wave mode with energy E , one has that

$$\begin{aligned} & \text{(Probability for a black hole to emit a particle in this mode)} \\ &= \exp\left(-\frac{E}{T_h}\right) \times \text{(Probability for a black hole to absorb a particle in the same mode),} \end{aligned}$$

where T_h is given by eqn. (28). The above relation was first obtained by Hartle and Hawking [36] using semiclassical analysis. Neglecting back-reaction, detailed balance condition requires that the ratio of the probability of having N particles in a particular mode to the probability of having $N - 1$ particles in the same mode is $\exp\left(-\frac{E}{T_h}\right)$. The argument in [31] gives the von Neumann entropy s_E for the mode

$$s_E = s\left(\frac{E}{T_h}\right), \quad (45)$$

where we define

$$s(x) = \frac{(-1)^\epsilon \exp x}{\exp x - (-1)^\epsilon} \ln \left[\frac{\exp x}{\exp x - (-1)^\epsilon} \right] + \frac{\ln [\exp x - (-1)^\epsilon]}{\exp x - (-1)^\epsilon}. \quad (46)$$

Note that $\epsilon = 0$ for bosons and $\epsilon = 1$ for fermions. As discussed in section III, it is interesting to note that there is an upper bound $m_p x_{cr}$ on the energy E of the particle.

For a Schwarzschild black hole, a wave mode of emitted scalars can be labelled by the energy E , angular momentum l , and magnetic quantum number m . Thus, the atmosphere entropy of a massless scalar field can be expressed in the form of

$$S_{rad} = \int (2l+1) dl \int_0^{E_{\max}} dE \frac{dn(E, l)}{dE} s_E, \quad (47)$$

where $E_{\max} = m_p x_{cr}$, and $n(E, l)$ is the number of one-particle states not exceeding E with fixed value of angular momentum l . To obtain $n(E, l)$, we can define the radial wave number $k(r, l, E)$ by

$$k^\pm(r, l, \omega) = p_r^\pm, \quad (48)$$

as long as $p_r^{\pm 2} \geq 0$, and $k^\pm(r, l, E) = 0$ otherwise. Note that p_r^\pm are given in eqn. (23), and $\lambda = (l + \frac{1}{2})^2 \hbar^2$ there for the Schwarzschild black hole[31]. With these two Dirichlet boundaries, one finds[24] that $n(E, l)$ is

$$n(E, l) = \frac{1}{2\pi\hbar} \left[\int_{r_h+r_\varepsilon}^L k^+(r, l, E) dr + \int_L^{r_h+r_\varepsilon} k^-(r, l, E) dr \right]. \quad (49)$$

Defining

$$u \equiv \frac{E}{T_h} = \frac{E}{T_0} \frac{f^3(E/m_p)}{g^3(E/m_p)}, \quad (50)$$

we can use eqns. (31) and (32) to show that

$$\frac{g(E/m_p)}{f(E/m_p)} = h^{\frac{1}{3}} \left(\frac{u T_0}{m_p} \right). \quad (51)$$

Thus, eqn. (47) becomes

$$\begin{aligned} S_{rad} &= \frac{1}{\hbar^2} \int_0^{u_{\max}} du s(u) \frac{d}{du} \left[\int d\lambda n(u, \lambda) \right] \\ &= \frac{2T_0^3}{3\pi\hbar^3} \int_0^{u_{\max}} du s(u) \frac{d}{du} \left[\int_{r_h+r_\varepsilon}^L dr \frac{r^2 u^3 h^{\frac{10}{3}} \left(\frac{u T_0}{m_p} \right)}{\left[B(r) + h^{\frac{2}{3}} \left(\frac{u T_0}{m_p} \right) - 1 \right]^2} \right], \end{aligned} \quad (52)$$

where $u_{\max} = \frac{m_p y_{cr}}{T_0}$ and $\lambda = (l + \frac{1}{2})^2 \hbar^2$.

Since the spacetime has a rainbow metric, it is natural that the position of the brick wall is energy dependent, just like the radius of the event horizon r_h . In this sense, in eqn. (52) the u derivative acts on not only the integrand of the integral in the square bracket, but also the lower limit $r_h + r_\varepsilon$. Focusing on the possible most divergent parts near the horizon, we have for the atmosphere entropy

$$\begin{aligned}
S_{rad} \sim & \frac{M}{16\pi^4} \int du u^2 s(u) h^{-\frac{2}{3}} \left(\frac{uT_0}{m_p} \right) \left[1 - \frac{10T_0 u}{9m_p} h' \left(\frac{uT_0}{m_p} \right) h^{-1} \left(\frac{uT_0}{m_p} \right) \right] \frac{1}{r_\varepsilon} \\
& - \frac{1}{24\pi^4} \int dus(u) u^3 \frac{1}{r_\varepsilon} \frac{dr_h}{du} + \frac{M}{48\pi^4} \int dus(u) u^3 h^{-\frac{2}{3}} \left(\frac{uT_0}{m_p} \right) \frac{d}{du} \left(\frac{1}{r_\varepsilon} \right) \\
& - \frac{M}{288\pi^5} \int du u^3 s(u) h^{-\frac{7}{3}} \left(\frac{uT_0}{m_p} \right) h' \left(\frac{uT_0}{m_p} \right) \frac{m_p}{r_\varepsilon^2} - \frac{M}{48\pi^4} \int dus(u) u^3 h^{-\frac{2}{3}} \left(\frac{uT_0}{m_p} \right) \frac{dr_h}{du} \frac{1}{r_\varepsilon^2}.
\end{aligned} \tag{53}$$

It would appear that the most divergent terms are these proportional to r_ε^{-2} . However, it can be shown from eqn. (27) that the two terms in the last line of eqn. (53) cancel against each other, leaving only the most divergent terms proportional to r_ε^{-1} .

To determine how r_ε depends on E , one could introduce the proper length for r_ε in the rainbow metric (11):

$$\varepsilon = \int_{r_h}^{r_h+r_\varepsilon} \sqrt{g_{rr}} dr = \frac{r_\varepsilon}{g(E/m_p)}. \tag{54}$$

Now consider the AC dispersion relation where $f(x) = 1$. In this case, eqn. (51) gives

$$\varepsilon = r_\varepsilon \frac{f(E/m_p)}{g(E/m_p)} = r_\varepsilon h^{-\frac{1}{3}} \left(\frac{uT_0}{m_p} \right). \tag{55}$$

One natural assumption is that ε does not depend on E . Under this assumption, the most divergent part of the atmosphere entropy near the horizon becomes

$$S_{rad} \sim \frac{M}{16\pi^4 \varepsilon} \int_0^{u_{\max}} du \frac{u^2 s(u)}{h \left(\frac{uT_0}{m_p} \right)} - \frac{1}{384\pi^5} \frac{m_p}{\varepsilon} \int_0^{u_{\max}} d\tilde{u} \frac{u^3 s(u) h' \left(\frac{uT_0}{m_p} \right)}{h^2 \left(\frac{uT_0}{m_p} \right)}. \tag{56}$$

Since ε is assumed to be independent of E , one way to understand the value of ε is letting S_{rad} recover the Bekenstein-Hawking entropy in the usual case, where $h(x) = 1$ and $u_{\max} = \infty$. Thus, we have for ε

$$\varepsilon = \frac{\hbar}{720\pi M}. \tag{57}$$

In this case, for $M \gg m_p$ eqn. (56) becomes

$$S_{rad} \sim \frac{A}{4\hbar} + \frac{45(3+n)\eta}{128\pi^5} \left(\frac{4\pi A}{\hbar} \right)^{\frac{2-n}{2}} \int_0^\infty dus(u) u^{n+2}, \tag{58}$$

where use eqn. (37) for $h(x)$. From eqns. (43) and (58), it shows that the leading rainbow corrections to S_{BH} and S_{rad} are both proportional to $A^{\frac{2-n}{2}}$ in the cases with $n \neq 2$. However, the logarithmic divergence does not appear in S_{rad} for the $n = 2$ case, which would imply that atmosphere entropy could not solely account for the entropy of the black hole.

V. DISCUSSION AND CONCLUSION

In [30], the thermodynamics of a SF rainbow Schwarzschild black hole was considered. The minimum masses M_{cr} and final temperatures T_{BH}^{cr} for the AC dispersion relation with different values of η and n were listed in TABLE II. Comparing with TABLE I, we find that the behaviors of SF and FF rainbow Schwarzschild black holes during the final stage of evaporation process are different for the scenarios with $\eta < 0$ and $\frac{2}{3} \leq n \leq 2$. Specifically, in the case with $\eta < 0$ and $n = \frac{2}{3}$, a remnant exists for the FF black hole while it does not for the SF one. In the case with $\eta < 0$ and $\frac{2}{3} < n < 2$, $M_{cr} > 0$ and T_{BH}^{cr} is finite for the FF black hole while $M_{cr} = 0$ and $T_{BH}^{cr} = \infty$ for the SF one. In the case with $\eta < 0$ and $n = 2$, both SF and FF black holes have remnants in their final stages while T_{BH}^{cr} is finite for the FF one and infinity for the SF one. On the other hand, TABLES I and II show that the behavior of a FF rainbow black hole appears amazingly similar to that of a SF one, except for the values of n at which stable remnants occur. For a SF black hole, the remnant occurs at somewhat higher values of n . These similarities show that the black hole thermodynamics in the rainbow gravity is kind of independent of the frames used to obtain the rainbow metrics, which hints that the Gravity's rainbow scenario has some degree of universality.

	M_{cr}	T_{BH}^{cr}/m_p
$\eta = 0$	0	∞
$\eta > 0$	0	$\frac{\eta^{-1/n}}{4\pi}$
$\eta < 0, 0 < n < 2$	0	∞
$\eta < 0, n = 2$	$\frac{m_p \eta ^{\frac{1}{2}}}{2}$	∞
$\eta < 0, n > 2$	$\frac{m_p}{2y_0}$	$\frac{\tilde{x}_0}{4\pi}$

TABLE II: The values of M_{cr} and T_{BH}^{cr}/m_p for a SF rainbow Schwarzschild black hole.

In this paper, we considered FF rainbow black holes, and analyzed the effects of rainbow gravity on the temperature, entropy and atmosphere entropy of a FF rainbow Schwarzschild black hole. After the metric of a FF rainbow black hole were proposed, we then used the Hamilton-Jacobi method to compute the effective Hawking temperature T_{eff} of the rainbow black hole, which depends on the energy E of emitted particles. By relating the momentum p of particles to the event horizon radius r_h of the black hole, the temperature of a FF rainbow Schwarzschild black hole was obtained. Focusing on the AC dispersion relation, we computed their minimum masses M_{cr} and final temperatures T_{BH}^{cr} for different values of η and n . All the results were listed in TABLE I. In addition, a non-vanishing minimum mass indicates the existence of the black hole's remnant, which could shed light on the "information paradox". In section IV, the atmosphere entropy of a massless scalar field in a FF rainbow Schwarzschild metric was calculated in the brick wall model.

Acknowledgments

We are grateful to Houwen Wu and Zheng Sun for useful discussions. This work is supported in part by NSFC (Grant No. 11005016, 11175039 and 11375121) and the Fundamental Research Funds for the Central Universities.

-
- [1] G. Amelino-Camelia, "Testable scenario for relativity with minimum length," *Phys. Lett. B* **510**, 255 (2001) [hep-th/0012238].
 - [2] G. Amelino-Camelia, "Relativity in space-times with short distance structure governed by an observer independent (Planckian) length scale," *Int. J. Mod. Phys. D* **11**, 35 (2002) [gr-qc/0012051].
 - [3] J. Magueijo and L. Smolin, "Lorentz invariance with an invariant energy scale," *Phys. Rev. Lett.* **88**, 190403 (2002) [hep-th/0112090].
 - [4] J. Magueijo and L. Smolin, "Generalized Lorentz invariance with an invariant energy scale," *Phys. Rev. D* **67**, 044017 (2003) [gr-qc/0207085].

- [5] G. Amelino-Camelia, J. R. Ellis, N. E. Mavromatos, D. V. Nanopoulos and S. Sarkar, “Tests of quantum gravity from observations of gamma-ray bursts,” *Nature* **393**, 763 (1998) [astro-ph/9712103].
- [6] D. Colladay and V. A. Kostelecky, “Lorentz violating extension of the standard model,” *Phys. Rev. D* **58**, 116002 (1998) [hep-ph/9809521].
- [7] S. R. Coleman and S. L. Glashow, “High-energy tests of Lorentz invariance,” *Phys. Rev. D* **59**, 116008 (1999) [hep-ph/9812418].
- [8] G. Amelino-Camelia and T. Piran, “Planck scale deformation of Lorentz symmetry as a solution to the UHECR and the TeV gamma paradoxes,” *Phys. Rev. D* **64**, 036005 (2001) [astro-ph/0008107].
- [9] T. Jacobson, S. Liberati and D. Mattingly, “TeV astrophysics constraints on Planck scale Lorentz violation,” *Phys. Rev. D* **66**, 081302 (2002) [hep-ph/0112207].
- [10] T. A. Jacobson, S. Liberati, D. Mattingly and F. W. Stecker, “New limits on Planck scale Lorentz violation in QED,” *Phys. Rev. Lett.* **93**, 021101 (2004) [astro-ph/0309681].
- [11] G. Amelino-Camelia, J. R. Ellis, N. E. Mavromatos and D. V. Nanopoulos, “Distance measurement and wave dispersion in a Liouville string approach to quantum gravity,” *Int. J. Mod. Phys. A* **12**, 607 (1997) [hep-th/9605211].
- [12] G. Amelino-Camelia, “Quantum-Spacetime Phenomenology,” *Living Rev. Rel.* **16**, 5 (2013) [arXiv:0806.0339 [gr-qc]].
- [13] J. Magueijo and L. Smolin, “Gravity’s rainbow,” *Class. Quant. Grav.* **21**, 1725 (2004) [gr-qc/0305055].
- [14] Y. Ling, X. Li and H. b. Zhang, “Thermodynamics of modified black holes from gravity’s rainbow,” *Mod. Phys. Lett. A* **22**, 2749 (2007) [gr-qc/0512084].
- [15] P. Galan and G. A. Mena Marugan, “Entropy and temperature of black holes in a gravity’s rainbow,” *Phys. Rev. D* **74**, 044035 (2006) [gr-qc/0608061].
- [16] H. Li, Y. Ling and X. Han, “Modified (A)dS Schwarzschild black holes in Rainbow spacetime,” *Class. Quant. Grav.* **26**, 065004 (2009) [arXiv:0809.4819 [gr-qc]].
- [17] R. Garattini, “Modified Dispersion Relations and Black Hole Entropy,” *Phys. Lett. B* **685**, 329 (2010) [arXiv:0902.3927 [gr-qc]].
- [18] G. Salesi and E. Di Grezia, “Black hole evaporation within a momentum-dependent metric,” *Phys. Rev. D* **79**, 104009 (2009) [arXiv:0902.3763 [gr-qc]].

- [19] S. Esposito and G. Salesi, “Black hole dynamical evolution in a Lorentz-violating spacetime,” *Phys. Rev. D* **83**, 084043 (2011) [arXiv:1012.4180 [gr-qc]].
- [20] A. F. Ali, “Black hole remnant from gravity’s rainbow,” *Phys. Rev. D* **89**, no. 10, 104040 (2014) [arXiv:1402.5320 [hep-th]].
- [21] Y. Gim and W. Kim, “Thermodynamic phase transition in the rainbow Schwarzschild black hole,” *JCAP* **1410**, 003 (2014) [arXiv:1406.6475 [gr-qc]].
- [22] A. F. Ali, M. Faizal and M. M. Khalil, “Remnant for all Black Objects due to Gravity’s Rainbow,” *Nucl. Phys. B* **894**, 341 (2015) [arXiv:1410.5706 [hep-th]].
- [23] S. Corley and T. Jacobson, “Hawking spectrum and high frequency dispersion,” *Phys. Rev. D* **54**, 1568 (1996) [hep-th/9601073].
- [24] P. Wang, H. Yang and S. Ying, “Black Hole Radiation with Modified Dispersion Relation in Tunneling Paradigm: Free-fall Frame,” *Eur. Phys. J. C* **76** (2016) 1, 27 [arXiv:1505.04568 [gr-qc]].
- [25] P. Kraus and F. Wilczek, “Selfinteraction correction to black hole radiance,” *Nucl. Phys. B* **433**, 403 (1995) [gr-qc/9408003].
- [26] P. Kraus and F. Wilczek, “Effect of selfinteraction on charged black hole radiance,” *Nucl. Phys. B* **437**, 231 (1995) [hep-th/9411219].
- [27] K. Srinivasan and T. Padmanabhan, “Particle production and complex path analysis,” *Phys. Rev. D* **60**, 024007 (1999) [gr-qc/9812028].
- [28] M. Angheben, M. Nadalini, L. Vanzo and S. Zerbini, “Hawking radiation as tunneling for extremal and rotating black holes,” *JHEP* **0505**, 014 (2005) [hep-th/0503081].
- [29] R. Kerner and R. B. Mann, “Tunnelling, temperature and Taub-NUT black holes,” *Phys. Rev. D* **73**, 104010 (2006) [gr-qc/0603019].
- [30] B. Mu, P. Wang and H. Yang, “Thermodynamics and Luminosities of Rainbow Black Holes,” *JCAP* **1511**, no. 11, 045 (2015) [arXiv:1507.03768 [gr-qc]].
- [31] P. Wang and H. Yang, “Black Hole Radiation with Modified Dispersion Relation in Tunneling Paradigm: Static Frame,” arXiv:1505.03045 [gr-qc].
- [32] J. D. Bekenstein, “Black holes and entropy,” *Phys. Rev. D* **7**, 2333 (1973).
- [33] R. J. Adler, P. Chen and D. I. Santiago, “The Generalized uncertainty principle and black hole remnants,” *Gen. Rel. Grav.* **33**, 2101 (2001) [gr-qc/0106080].
- [34] J. Z. Simon, “Higher Derivative Lagrangians, Nonlocality, Problems and Solutions,” *Phys.*

- Rev. D **41**, 3720 (1990).
- [35] G. 't Hooft, “On the Quantum Structure of a Black Hole,” Nucl. Phys. B **256**, 727 (1985).
- [36] J. B. Hartle and S. W. Hawking, “Path Integral Derivation of Black Hole Radiance,” Phys. Rev. D **13**, 2188 (1976).